NeuroImage: Clinical 35 (2022) 103124

Contents lists available at ScienceDirect

NeuroImage: Clinical

journal homepage: www.elsevier.com/locate/ynicl

Spinal cord and brain tissue impairments as long-term effects of rugby practice? An exploratory study based on T_1 and ihMTsat measures

Arash Forodighasemabadi [a,b,c,d], Guillaume Baucher [a,b,e], Lucas Soustelle [a,b], Thomas Troalen [f], Olivier M. Girard [a,b], Maxime Guye [a,b], Jean-Baptiste Grisoli [g], Jean-Philippe Ranjeva [a,b], Guillaume Duhamel [a,b], Virginie Callot [a,b,d,*]

[a] Aix-Marseille Univ, CNRS, CRMBM, Marseille, France
[b] APHM, Hopital Universitaire Timone, CEMEREM, Marseille, France
[c] Aix-Marseille Univ, Université Gustave Eiffel, LBA, Marseille, France
[d] iLab-Spine International Associated Laboratory, Marseille-Montreal, France
[e] APHM, Hopital Universitaire Nord, Neurosurgery Dept, Marseille, France
[f] Siemens Healthcare SAS, Saint-Denis, France
[g] APHM, Hopital Universitaire Timone, Pôle MPR, Marseille, France

ARTICLE INFO

Keywords:
Rugby
Brain
Cervical spinal cord
T_1 MP2RAGE
Inhomogeneous magnetization transfer
Neurodegeneration

ABSTRACT

Rugby players are subject to multiple impacts to their head and neck that could have adverse neurological effects and put them at increased risk of neurodegeneration.

Previous studies demonstrated altered default mode network and diffusion metrics on brain, as well as more foraminal stenosis, disc protrusion and neck pain among players of contact sports as compared to healthy controls. However, the long-term effects of practice and repetitive impacts on brain and cervical spinal cord (cSC) of the rugby players have never been systematically investigated.

In this study, 15 retired professional and amateur rugby players (R) and 15 age-matched healthy controls (HC) (all males; mean age R: 46.8 ± 7.6; and HC: 48.6 ± 9.5) were recruited both to investigate cord impairments and further characterize brain structure damage. Medical questionnaires including modified Japanese Orthopedic Association scale (mJOA) and Neck Disability Index (NDI) were filled by all participants. A 3 T multi-parametric MR protocol including conventional qualitative techniques such as T_1-, T_2-, and T_2*-weighted sequences, as well as state-of-the art quantitative techniques including MP2RAGE T_1 mapping and 3D ihMTRAGE, was used on both brain and cSC. Normalized brain WM and GM volumes, spine Overall Stenosis Score, cord cross-sectional area and regional T_1 and ihMT metrics were derived from these acquisitions.

Rugby players showed significantly higher NDI scores, as well as a faster decline of normalized brain GM volume with age as compared to HC. Moreover, higher T_1 values on cSC suggestive of structural degeneration, together with higher T_1 and lower ihMTsat on brain WM suggestive of demyelination, were observed in retired rugby players as compared to age-matched controls, which may suggest cumulative effects of long-term impacts on the tissues. Metrics also suggest early aging and different aging processes on brain tissue in the players.

These preliminary observations provide new insights in the domain, which should now be further investigated on larger cohorts and multicentric longitudinal studies, and further correlated to the likelihood of neurodegenerative diseases and risk factors.

Abbreviations: CSA, Cross-Sectional Area; cSC, Cervical Spinal Cord; CSF, Cerebrospinal Fluid; CST, Corticospinal Tracts; GM, Gray Matter; HC, Healthy Control; ihMT, inhomogeneous Magnetization Transfer; LST, Lateral Sensory Tracts; mJOA, Modified Japanese Orthopedic Association; MP2RAGE, Magnetization Prepared 2 Rapid Acquisition Gradient Echo; NDI, Neck Disability Index; OSS, Overall Stenosis Score; PST, Posterior Sensory Tracts; R, Rugby player; RST, Reticulo/Rubrospinal Tracts; WM, White Matter.

* Corresponding author at: CRMBM-CEMEREM, UMR 7339, CNRS - Aix-Marseille Université, Faculté de Médecine, 27, bd Jean Moulin, 13385 Marseille Cedex 5, France

E-mail address: virginie.callot@univ-amu.fr (V. Callot).

https://doi.org/10.1016/j.nicl.2022.103124
Received 18 March 2022; Received in revised form 14 July 2022; Accepted 20 July 2022
Available online 23 July 2022

1. Introduction

Players of contact sports, such as rugby, receive repetitive impacts to their head and neck that do not necessarily result in observable injuries (Bathgate et al., 2002). However, there have been several studies demonstrating the adverse effects of these impacts on the health of players. Most of these studies, focusing on the brain, demonstrated that rugby players, even without a history of concussion, may present lower visuomotor processing speed (Shuttleworth-Rdwards and Radloff, 2008), more cognitive vulnerability (Alexander et al., 2015) and longer reaction times (Hume et al., 2017) compared to age-matched controls. Diffusion Tensor Imaging (DTI) and functional MRI (fMRI) studies on brain have also demonstrated impaired microstructure with decreased Fractional Anisotropy (FA) in multiple white matter (WM) tracts accompanied with default mode network and visual network hyper-connectivity in rugby players in-season as compared to off-season, which was not observed in players of non-contact sports (Manning et al., 2020). On spine, rugby players were found to have more chronic neck pain and foraminal stenosis, narrower vertebral canal, and more substantial osteophytes as compared to age-matched healthy controls (Berge et al., 1999; Brauge et al., 2015). However, no studies have been conducted so far to characterize potential effects on the cervical spinal cord (cSC) itself.

In this study, we propose to use complementary state-of-the-art quantitative MRI techniques that have been recently adapted to brain and SC imaging at 3 T to scan retired rugby players that have played in amateur and professional leagues. The protocol included a fast 3D Magnetization Prepared 2 Rapid Acquisition Gradient Echo (MP2RAGE) T_1 mapping of both brain and cervical cord (Forodighasemabadi et al., 2021), as well as the recent 3D inhomogeneous Magnetization Transfer with rapid acquisition gradient echo technique (ihMTRAGE) (Varma et al., 2020). Conventional T_1 relaxometry has already been used widely to study tissue alterations in pathologies such as Multiple Sclerosis (MS) or Parkinson's disease (PD) (Haacke et al., 2005; Sian-Hülsmann et al., 2011; Paul, 2016), where it was demonstrated to be sensitive to demyelination, iron deposition or structural variations. Interestingly demyelination and iron accumulation could affect T_1 in opposite directions (Stüber et al., 2014), T_1 could therefore lack specificity if both phenomena are present. The ihMT method, on the other hand, is more specific to myelin in central nervous system (CNS) tissues (Varma et al., 2015; Girard et al., 2015; Varma et al., 2015; Duhamel et al., 2019). It has been used in several clinical and preclinical studies on brain (Varma et al., 2015; Varma et al., 2015; Prevost et al., 2017; Mchinda et al., 2018; Van Obberghen et al., 2018; Munsch et al., 2020; Geeraert et al., 2017; Ercan et al., 2018) and recently adapted to SC imaging to study demyelinating pathologies such as MS and normal aging (Girard et al., 2017; Taso et al., 2016; Rasoanandrianina et al., 2020; Rasoanandrianina et al., 2017).

By comparing brain and cSC T_1 and ihMT metrics collected on both retired players and age-matched healthy controls, this work investigated whether the cord is impaired and early tissue aging occurs in the rugby player population, while refining previously reported brain tissue structure damage description. Table 1.

2. Materials & Methods

2.1. Subjects and clinical assessments

Fifteen retired rugby players (all males; 7 professionals and 8 amateurs) without known neurodegenerative disease and with no prior cervical spine surgery were enrolled in the study, together with 15 aged- and sex-matched healthy controls. Demographic data are summarized in Table 2. The local ethics committee of our institution approved the protocol and written informed consent was obtained from each participant.Table 3..

Modified Japanese Orthopedic Association score (mJOA) (Association, 1996) and neck pain (Neck Disability Index (NDI)(Vernon and Mior, 1991) questionnaires were filled by the participants to evaluate motor and sensory dysfunction.

2.2. MR protocol

The subjects were scanned with a multi-parametric MR protocol using a 3 T MR system (MAGNETOM Vida, Siemens Healthcare, Erlangen, Germany) with a 20-channel head and neck coil. Neck and brachial plexus MRI pads (Sat Pad Clinical Imaging Solutions, West Chester, PA, USA) were installed around the subject's neck and shoulders to reduce the B_0 magnetic field inhomogeneity. When possible for the subject, the

Table 1
Multi-parametric MR protocol used for the study and derived metrics. TSE: Turbo Spin Echo; SPACE: Sampling Perfection with Application-optimized Contrasts using different flip angle Evolution (Siemens); MGE: Multi Gradient Echo; FLAIR: FLuid-Attenuated Inversion Recovery; CSA: Cross-Sectional Area; GM: Gray Matter; WM: White Matter.

Sequence	Region	Orientation	Resolution (mm^3)	TR (s)	FOV (mm^2)	Acq. Time (min)	Information / MR metrics of interest
T_2w TSE	SC	SAG	0.6 × 0.6 × 3	3500	220 × 220	1:47	Disc protrusion
T_2w SPACE	SC	SAG	0.6 × 0.6 × 1	1500	256 × 256	2:42	Antero-posterior and right-left diameter of cord and canal; Foraminal stenosis
T_2*w MGE	SC	TRA	0.4 × 0.4 × 5	1400	180 × 180	5:04	GM, WM, and SC CSA
T_2w FLAIR	Brain	TRA	0.9 × 0.9 × 5	10,000	240 × 180	2:42	Investigating (lack of) major brain abnormalities
Presat TFL	SC + Brain	SAG	5 × 5 × 5	5000	320 × 320	10 s	B_1^+ map used to correct T_1 and ihMT-bias
ihMT RAGE	SC	TRA	0.9 × 0.9 × 10	2500	180 × 180	9:47	ihMTsat maps
	Brain		2 × 2 × 2		256 × 200	13:34	
	Specific parameters Low Duty Cycle (DC) high RF power ihMT preparation: train of ten 5 ms-pulses (Tukey-shaped pulses with a cosine fraction (Harris, 1978) of r = 0.2 ; B_1-peak = 14.13 μT; Cosine-modulated pulses for the dual-offset saturation (Varma et al., 2020;(April):mrm.28324.; Munsch et al., October 2020); repeated every 100 ms (DC = 5 %); total saturation time 1 s; B_1-RMS = 2.95 μT; frequency offset (f) 7 kHz. Five volumes on brain: M0, MT+, MT±, MT-, MT ± and 13 volumes on SC: M0 + 3 repetitions of (MT+, MT±, MT-, $MT_\pm$).						
MP2RAGE	Brain + SC (single acquisition)	SAG	0.9 × 0.9 × 0.9	6.2	315 × 258	8:02	T_1 quantitative maps; Normalized GM/WM volume
	Specific parameters TI1/TI2/α_1/α_2 = 650 ms/3150 ms/5°/3°; GRAPPA = 2; Partial Fourier = 6/8; MP2RAGE TR 4000 ms						

Table 2
Demographic data, NDI and mJOA scores, and overall stenosis score (OSS); **: p-value < 0.01.

	Retired Rugby Players (R)	Healthy controls (HC)
Number of participants	15	15
Players in front / second / third row position	8 / 4 / 3	–
Mean age (years old (yo)) [min, median, max]	46.8 ± 7.6	48.6 ± 9.5
Mean rugby practice duration (yo)	26.2 ± 9.5	–
Mean duration from rugby practice retirement (yo)	9.8 ± 5.4	–
Clinical scoring		
mJOA (/17)	16.7 ± 0.5	17
NDI (%) [min, median, max]	**9.4 ± 7.2** ** [0, 8, 30]	**4 ± 8.7** [0, 0, 34]
OSS [min, median, max]	1.8 ± 0.8	1.9 ± 1.1 [0, 2, 4]

mJOA, from 0 to 17, with values between 15 and 17 considered as mild degeneration and ≤ 14 as moderate-to-severe (Association, 1996); NDI, from 0 to 50; also expressed from 0 to 100 %, with values < 8 %, < [10–28 %], and [30–48 %] considered as normal, mild and moderate disability, respectively (Vernon and Mior, 1991); OSS, from 0 to 18, defined as the sum of stenosis score at each level (*C*2-3 to C6-C7 and C1) in a range of 0 to 3 for normal, mildly, moderately, or severely compressed, respectively.

Table 3
The mean ± inter-subject SD of T_1 and ihMTsat in rugby players (R) and healthy controls (HC) in different ROIs of SC and brain (see Fig. 1). *: p-value < 0.05, ***: p-value < 0.001. The p-values correspond to the MANOVA test performed on each ROI and corrected for multiple analyses (different ROIs, 2 parameters) on brain and SC, separately.

qMRI		T_1 (ms)		ihMTsat (%)	
SC ROI		R	HC	R	HC
WM	CST	**929.7 ± 26.5***	917.3 ± 25.7	3.2 ± 0.1	3.2 ± 0.2
	PST	953.5 ± 27.6	941.1 ± 33	3.3 ± 0.2	3.3 ± 0.3
	RST	**919 ± 25.1*****	901.4 ± 25.2	3.2 ± 0.1	3.2 ± 0.2
___	LST	**925 ± 34.2***	911.9 ± 27.7	3.1 ± 0.2	3.1 ± 0.2
GM	ant-int	**978.7 ± 23.3***	967.6 ± 19.5	3.0 ± 0.1	3.0 ± 0.2
Brain ROI					
WM		830.8 ± 17.3	817.9 ± 21.6	3.3 ± 0.1	3.4 ± 0.1
GM		1315.3 ± 26.8	1307.7 ± 19.1	1.2 ± 0.1	1.2 ± 0.1
dGM		1130.7 ± 28.2	1130.1 ± 29.7	1.4 ± 0.1	1.4 ± 0.1

RF coil was tilted to place the cord as straight as possible and hence minimize partial volume effects (PVE) encountered with non-isotropic sequences due to the cord curvature.

The multi-parametric MRI protocol included conventional anatomical techniques, as well as quantitative MP2RAGE (Forodighasemabadi et al., 2021) and ihMTRAGE (Varma et al., 2020) sequences, as detailed in Table 1. T_2* and ihMT slices were placed perpendicular to the cord to minimize PVE. The MP2RAGE and ihMT techniques are detailed in the following sections. The protocol also included a B_1^+ map acquired using a pre-saturated turbo flash (TFL) sequence (Chung et al., 2010) to correct quantitative T_1 values and ihMT signal from B_1^+ inhomogeneities (see below). The whole protocol lasted 50 min.

2.2.1. Magnetization Prepared 2 Rapid acquisition Gradient Echo

MP2RAGE is an Inversion Recovery (IR)-based technique that acquires two RAGE volumes in an interleaved manner, from which a uniform (UNI) image is derived, which can then be used to estimate the T_1 of the tissue voxel-wise. Originally proposed for the brain (Marques et al., 2010) and widely used to study pathologies like MS (Kober et al., 2012; Okubo et al., 2016; Marques and Gruetter, 2013; Simioni et al., 2014), this technique was then optimized to study healthy and pathological cervical cord (Massire et al., 2016; Rasoanandrianina et al., 2019; Demortière et al., 2020; Baucher et al., 2021). Recently tuned at 3 T with regards to CNR and B_1^+ insensitivity to study both brain and cSC simultaneously (Forodighasemabadi et al., 2021), this latter setup was used in the present study. Potential T_1 imperfections due to residual B_1^+ inhomogeneities were corrected using a B_1^+ map as in (Massire et al., 2016).

2.2.2. Inhomogeneous Magnetization Transfer

IhMT has recently been proposed and validated as a myelin sensitive and specific technique (Varma et al., 2015; Girard et al., 2015; Varma et al., 2015; Duhamel et al., 2019). The ihMT image is generated by the subtraction of a MT weighted image acquired with a single frequency irradiation (MT_{sing}) and one acquired with power evenly split between positive and negative frequency offsets ($MT_{\pm}$) (Girard et al., 2017). In practice, to limit the effects of MT asymmetry (Prevost et al., 2016), the single frequency image MT_{sing} is obtained by adding an image at the positive frequency (MT_{+}) and one at the negative frequency (MT.) such that $MT_{sing} = MT_{+}$+MT.. Hence, for consistency, the dual offset image is acquired twice such that the ihMT image is given by ihMT= ($MT_{+} + MT. - 2\ MT_{\pm}$).

Several variants of the ihMT technique have been proposed in the past, including single slice 2D ihMT-HASTE (Half-Fourier Acquisition Single-shot Turbo spin Echo) for brain (Girard et al., 2015) and SC (Girard et al., 2017; Taso et al., 2016; Rasoanandrianina et al., 2020); 3D ihMT-GRE for brain (Mchinda et al., 2018) and multi-slice ihMT SE-*EPI* for SC (Rasoanandrianina et al., 2017:p.0912.; Rangwala et al., 2013: p.350.). In this study, a 3D ihMT-RAGE sequence initially proposed for brain (Varma et al., 2020), and recently adapted to cervical spinal cord imaging (Troalen et al., 2018; Forodighasemabadi et al., 2020:p.1175.) was used. The preparation scheme (Table 1) was similar to (Varma et al., 2020; Munsch et al., 2020) and used identically for both the brain and SC. Note however, that the spatial resolution and the number of repetitions differed. IhMTsat metrics, corrected for T_1-relaxation and B_1^+-inhomogeneities that can bias regular ihMTR values (with ihMTR defined as $ihMT/2M_0$) at 3 T (Forodighasemabadi et al., 2020; Varma et al., 2019), were derived based on a strategy recently customized for the ihMTRAGE framework (Munsch et al., 2020) (see 2.4 section).

2.3. Morphological measurements

Discal cross-sectional areas, as well as antero-posterior and right-left diameters of canal and cord were manually measured by an experienced neurosurgeon for each subject using the Horos software (horosproject.org), based on T_2 SPACE image (intra-rater reproducibility: 3.6 %, 4.6 %, 5.1 %, 4.0 %, 5.8 %, and 7.6 %, for canal AP diameter, canal RL diameter, SC AP diameter, SC RL diameter, canal CSA, and SC CSA, respectively). Cord-to-canal (CCR) and canal occupation (COR) ratios were subsequently derived (see definition in Table S1). The degree of stenosis (see definition in Table 2) was assessed in the meantime using the same contrast. Fig. S1

The axial T_2*-weighted MGE images were used for the automatic segmentation of GM, WM, and SC using the SCT (De Leener et al., 2016) *deepseg* tool, from which mean CSAs were estimated at each level.

Finally, the UNI image (derived from MP2RAGE technique) was brain-extracted and segmented into GM, WM, and cerebrospinal fluid (CSF) using SPM12 (https://fil.ion.ucl.ac.uk/spm) "*New segment*" tool (Ashburner and Friston, 2005). The volumes of brain GM and WM were each normalized by the intracranial content (GM + WM + CSF) to remove inter-subject differences and investigate variation with age.

2.4. T_1 And ihMTsat post-processing

The post-processing steps to provide regional T_1 and ihMTsat measurements are depicted in Fig. 1.

All MT-weighted volumes (MT_{+}, MT., $MT_{\pm}$) of the ihMT-RAGE images acquired on SC and brain were motion-corrected by SCT (De Leener et al., 2016) *MoCo* and *ihMT-MoCo* (Soustelle et al., 2020), respectively. After motion correction, the MT-weighted volumes on SC and brain were

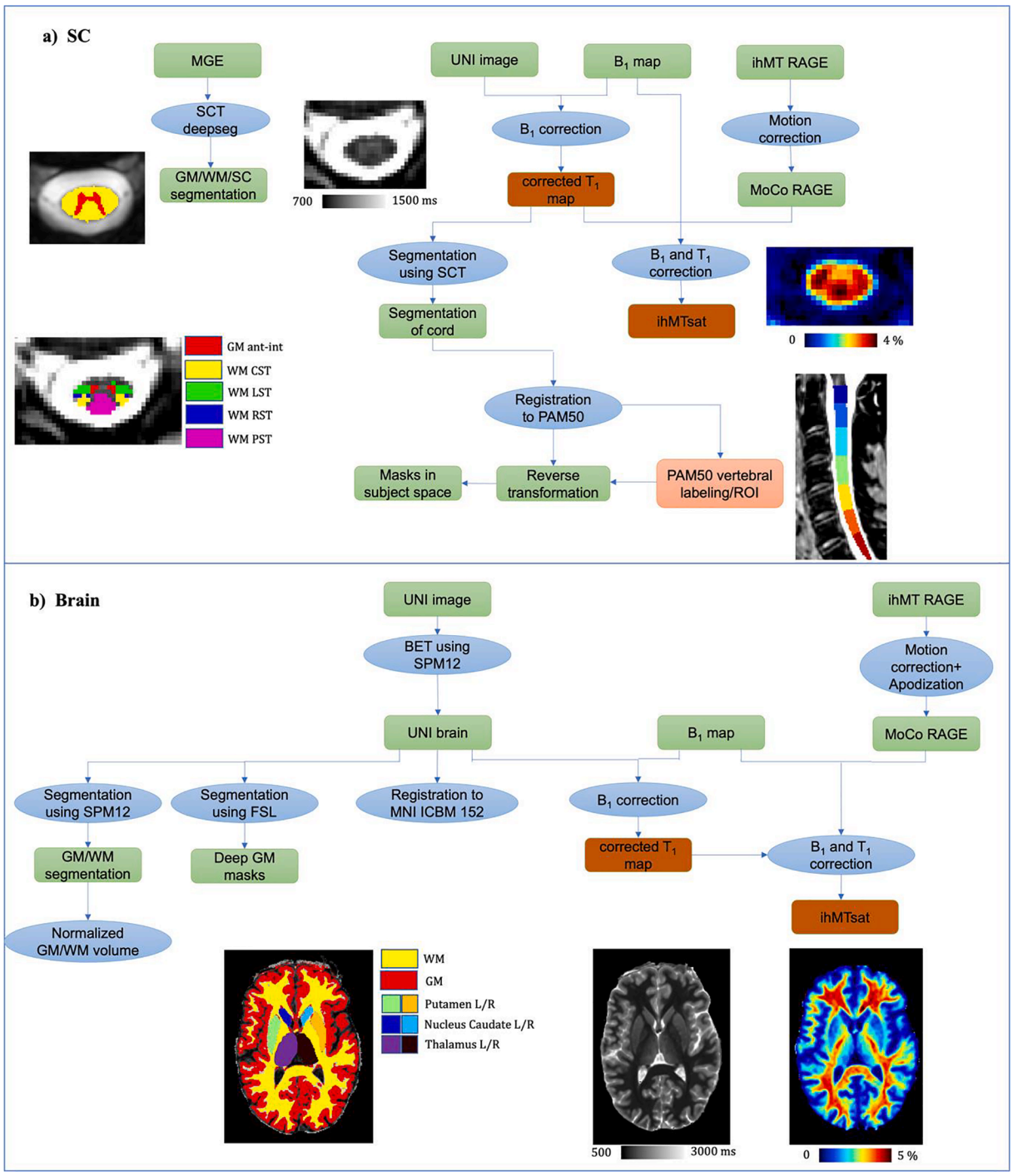

Fig. 1. Main post-processing steps (motion correction, B_1^+ and/or T_1 bias-correction, registration and segmentation, ROI labeling) for MP2RAGE and ihMT images on both a) SC and b) brain. (ROIs on SC: GM ant-int: anterior and intermediate; WM CST: corticospinal tracts; LST: lateral sensory tracts; RST: rubro/reticulospinal tracts; PST: posterior sensory tracts).

registered to their respective T_1 maps using SCT *multi-modal registration* and syN-ANTS (Helms et al., 2008) rigid registration tools, respectively. As previously mentioned, the ihMTR was not used in this study, instead the ihMTsat metric was calculated. The reader can refer to Munsch et al (Munsch et al., 2020). Briefly, the derivation of ihMTsat approach (Munsch et al., 2020) relies on a model that describes the effect of each RF saturation pulse as a fractional attenuation (δ) of the free water pool (e.g. the free pool magnetization right after a dual-offset RF pulse ($MT_{\pm}$') is related to the magnetization right before ($MT_{\pm}$) by $MT_{\pm}'=(1-\delta_{M\pm}) \times MT_{\pm}$). B_1 and T_1 maps were used to determine the δ factors that fit the attenuation of each MT-w relative to the unsaturated M_0 image, given the ihMTRAGE sequence parameters. The ihMTsat metric was finally derived from to the formulae (Munsch et al., 2020):

$$ihMTsat = (2\delta_{MT\pm} - \delta_{MT+} - \delta_{MT-}) \times \left(\frac{B_{1nom}}{B_{1act}}\right)^2$$

Where the term $\left(\frac{B_{1nom}}{B_{1act}}\right)^2$ that accounts for the quadratic B_1 dependence of ihMT with the saturation parameters used (Varma et al., 2018) corrects for B_1 inhomogeneities. B_{1nom} and B_{1act} represent the nominal

and actual pulse amplitudes calculated from the B_1^+ map. The post-processing pipeline for ihMTsat maps derivation is available in: https://github.com/lsoustelle/ihmt_proc (hash f3f49e0)).

The T_1 maps were then non-linearly registered to the ICBM-MNI-152 (Fonov et al., 2009; Fonov et al., 2011) template on brain and PAM50 template on SC (De Leener et al., 2017). On SC, the PAM50 regions of interest including WM Corticospinal Tracts (CST), Lateral Sensory Tracts (LST), Posterior Sensory Tracts (PST), Rubro/Reticulospinal Tracts (RST), and anterior and intermediate GM (ant-int) were warped back into the subject space and used for quantification of the quantitative maps. On brain, in addition to WM and cortical GM compartments, deep GM structures including Thalamus, Nucleus Caudate, and Putamen were segmented using FSL *FIRST* tool (https://fsl.fmrib.ox.ac.uk/) (Patenaude et al., 2011). The brain maps were quantified for each of these compartments and deep GM regions.

2.5. Statistical analyses

The statistical analyses were performed using JMP Version 9 (SAS Institute Inc., Cary, NC).

The mJOA and NDI scores were compared between the rugby players and controls using the non-parametric Steel-Dwass all pairs test, separately, and a p-value < 0.05 was considered as statistically significant.

For SC, T_1 and ihMTsat parameters were compared between Rugby players and healthy controls using ANOVA, looking at the (R vs HC) group effect when accounting for age and cervical levels. P values were corrected for multiple comparisons (5 ROIs, 2 parameters, $p_{corrected} < 0.005$).

For the brain, T_1 and ihMTsat parameters were also compared between Rugby players and healthy controls in the three compartments using ANOVA, looking at the (R vs HC) group effect when accounting for age. P values were corrected for multiple comparisons (3 compartments, 2 parameters, $p_{corrected} < 0.008$).

To investigate the evolution of metrics with age, linear regressions were performed.

Finally, R_1 ($1/T_1$) and ihMTsat maps on brain and SC were used in voxel-wise multi-variate analyses using the Permutation Analysis of Linear Models (PALM) tool available in the FSL package (version alpha119) (Winkler et al., 2014). The Non-Parametric Combination (NPC) option (Winkler et al., 2016), which allows joint inference over multiple modalities, was more particularly used in this study. To benefit from the multi-parametric MR protocol, R_1 and ihMTsat maps were thus combined using NPC in order to locate potential tissue abnormalities and investigate whether R_1 and ihMTsat were significantly lower in players as compared to HC. For both brain and SC, the analysis was performed using WM mask, GM mask, and the whole structure. For the analysis, 5000 permutations were used, along with the Threshold Free Cluster Enhancement (TFCE) option. The results were corrected for Family-Wise Error (FWEP-corrected) and for multiple modalities. The threshold was then set at p-value < 0.05.

2.6. Data/code availability statements

Data can be made available via a request to the authors and will be shared through a formal data sharing agreement.

The post-processing code has been well described in the Materials & Methods section and Fig. 1, with all the software and toolboxes used (SCT, FSL, SPM, ANTS, etc.). The ihMTsat map derivation code is also available at: https://github.com/lsoustelle/ihmt_proc (hash f3f49e0)).

3. Results

3.1. Clinical assessment

All scores are summarized in Table 2. All rugby players and 13 HC presented at least one grade of canal stenosis. NDI were significantly higher in players than in controls (p-value < 0.005), but with values ranging from normal to mild disability. No significant differences were observed between the mJOA scores of players and HC, however, 3 amateur players presented mild alterations.

3.2. Morphological results

Morphological results are summarized in table S1 (supplementary data). No differences in SC and brain morphometrics were observed between rugby players and healthy controls. However, for cerebral GM compartment, one age $\times$ group interaction was observed (ANOVA $p < 0.03$) related to a significant negative correlation between normalized GM volume and age in rugby players ($p = 0.003$), not observed in controls. (Fig. 2a).

3.3. Quantitative imaging results

Representative images and quantitative T_1 and ihMTsat maps of both brain and SC obtained from one rugby player are provided on Fig. 3.

IhMT data biased from PVE due to cord curvature (visual assessment) were removed from the analysis (2, 2, 8, and 9 images for the C1, *C*2, C6, and C7 levels, respectively, for rugby players and 1, 1, 1, 7 and 8 images at C1, C2, C5, C6, and C7 levels for the HC). Brain ihMTsat maps of one rugby player and one HC were also removed because of motion artifacts. Conversely, brain and SC T_1 maps of all subjects were kept.

Mean maps of R_1 ($1/T_1$) and ihMTsat for both rugby players and HC groups (obtained by averaging all individual maps co-registered in the PAM50 and MNI-152 template spaces) are presented on Fig. 4. Rugby players globally presented lower R_1 (i.e. higher T_1) on SC, and a trend toward lower R_1 and ihMTsat on brain.

Mean T_1 and ihMTsat values in the different ROIs are summarized on table 3 for both brain and cord, and for the 2 groups. On all ROIs of SC, the T_1 values were significantly higher in players as compared to HC. No significant differences were observed on brain. Detailed values of the 2 metrics in various brain regions derived from ICBM-MNI-152 lobes atlas (Fonov et al., 2009; Fonov et al., 2011) and JHU ICBM-DTI-81 WM label atlas (Mori et al., 2008; Hua et al., 2008) are provided in Table S2 (supplementary data) for reference and readers who might be interested, but none of them reached statistical significance.

Fig. 5 shows the clusters obtained by the PALM multi-variate test (with R_1 and ihMTsat metrics and using brain WM mask), in which a significant decrease in R_1 and/or ihMTsat was observed in players as compared to controls. Labels of tracts in which the clusters are located were derived from the JHU white-matter tractography (Wakana et al., 2007) and ICBM-DTI-81 white-matter labels atlases (Mori et al., 2008; Hua et al., 2008). The same tests were done with GM mask on brain, and GM and WM masks on SC, but no significant clusters were found.

Finally, the linear regression plots of T_1 and ihMTsat values with age in different ROIs of brain and SC are given in Fig. 6. As shown from HC values (orange lines), T_1 increased with age in the normal population with statistical significance in brain WM regions (Fig. 6d, $p = 0.0006$), and ihMTsat decreased in brain WM (Fig. 6h, $p = 0.003$) and SC WM and GM regions (Fig. 6e and 6 g, $p \leq 0.02$). Different behaviors were observed for rugby players (blue lines): T_1 decreased slightly with age in SC GM (Fig. 6a) and brain WM (Fig. 6d), and significantly in brain GM (Fig. 6b, $p = 0.02$), with all initial values above those of HC. For ihMTsat, all initial values were below those observed in HC, values then remained fairly constant with age in brain and SC GM (Fig. 6e and 6f), and slightly decreased in brain and SC WM (with a slope almost divided by 2 as compared to HC, Fig. 6g and 6 h).

4. Discussion

While spine degeneration linked to rugby activity has been previously reported (Berge et al., 1999; Brauge et al., 2015), little is known about the spinal cord itself. Taking advantage of a multi-parametric MR

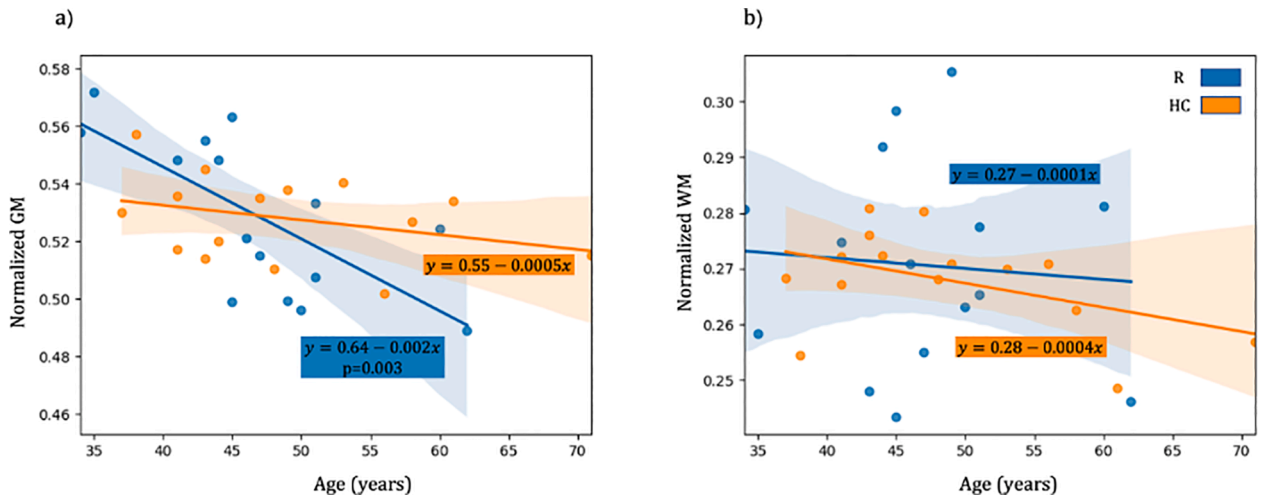

Fig. 2. Regression plots for (a) Normalized GM and (b) Normalized WM (on brain) volumes vs age, for Rugby players (R, blue) and Healthy Controls, (HC, orange). Age had a significant effect on the normalized GM volume in the rugby players group ($p = 0.003$) that was not observed in HC, nor in WM.

protocol including quantitative state-of-the-art T_1 MP2RAGE and ihMT techniques, both spinal cord and brain tissues from retired rugby players were analyzed in an attempt to characterize possible early aging and to refine tissue damage description. The global observations made between players and HC are summarized in Table 4. While brain and spine morphometrics were not largely affected in this population of retired rugby players, microstructure tissue damage was demonstrated, with deleterious effect of potential cumulative microtrauma highlighted with the multivariate voxel-wise approach, especially on cerebral WM tracts.

4.1. Clinical scoring and morphological variations

Previous studies on the cervical spine of former professional rugby players showed that players complained of chronic neck pain significantly more than controls, with more foraminal stenosis, narrower AP cord diameter, higher CCR, but no significant difference for clinical evaluations (JOA questionnaire, visual analog scale and NDI) (Berge et al., 1999; Brauge et al., 2015). Results from the present study, performed on a much smaller cohort, globally aligned with these observations (significantly higher NDI but ranging from normal to mild, slightly different AP diameter, canal stenosis, and higher CCR), nonetheless spine degeneration was not prominent in this population.

On the brain, cortical and cerebellar GM volumes were showed to reduce with age in the normal population (Taki et al., 2011; Jäncke et al., 2015). Here, the reduction in brain GM volume with age happened at a significantly faster rate for rugby players, which could indicate an early aging effect in brain GM linked to the rugby practice. However, the mean brain GM volume did not significantly differ between players and controls, thus requiring further study on larger cohorts and time points to better understand the tissue dynamic.

4.2. Quantitative MR metrics alterations

The potential microstructural alterations of the SC in players of contact sports have never been studied before, except in a preliminary investigative study relying on MP2RAGE and DTI that reported altered T_1 and DTI metrics in players ($n = 4$), especially in levels with disc protrusion (Rasoanandrianina, 2019). In our study and for the first time, these potential alterations were more largely investigated using both T_1 and ihMTsat. The higher T_1 values in GM and WM cSC regions observed in retired rugby players as compared to HC could demonstrate a diffuse microstructural alteration occurring as a result of rugby practice. However, the lack of difference in ihMTsat values between players and HC may indicate that the alterations are not necessarily related to demyelination or that alterations seen with ihMTsat could not be caught with the same sensitivity as in T_1. Future studies should focus on the sensitivity of each technique. It would also be interesting to combine MR investigation with biomechanical simulations (Rasoanandrianina, 2019) to further understand the effects of repetitive impacts on the spinal cord tissue and the presence of damage despite non prominent spine degeneration.

On brain, different studies have investigated the effects of sub-concussive impacts in athletes of contact sports. DTI and fMRI are among the tools commonly used to study these effects (Manning et al., 2020; Stamm et al., 2015). It was previously shown that football players demonstrated changes in their default mode network pre-season and post-season (Abbas et al., 2015), and that there was a relationship between age at first exposure to football and the white matter microstructure in professional players, which resulted in significant changes in DTI measures such as lower fractional anisotropy (FA) and higher radial diffusivity (RD) in anterior regions of corpus callosum (Stamm et al., 2015). One DTI study on ice hockey players also found that axial diffusivity (AD) and RD values in the right precentral region, right corona radiata, the anterior and posterior limb of the internal capsule and the superior longitudinal fasciculus were significantly different pre- and post-season (Koerte et al., 2012). Whereas these studies demonstrate the more acute and short-term effects of alterations in players of contact sports, our voxel-wise multi-variate analysis using both R_1 and ihMTsat showed significant clusters in identical brain regions such as corona radiata, internal capsule, superior and inferior longitudinal fasciculus, which could additionally indicate long term or persistent abnormalities that may be linked to the accumulating effect of impacts encountered in the rugby practice. The means of T_1 and ihMTsat in different ROIs of brain (table S2) show a similar (but non-significant) trend.

We also observed a significant decrease of T_1 with aging in brain GM of rugby players that could be indicative of excessive iron accumulation (together with a non-significant trend in SC GM). Iron is essential for a normal functioning brain, however impaired regulation can result in the production and accumulation of reactive oxygen species and cause oxidative stress that the biological system is not able to detoxify (Núñez et al., 2012; Daglas and Adlard, 2018). Iron accumulation occurs in brain GM with normal aging (del C. Valdés Hernández et al., 2015; Hagemeier et al., 2012), however, there is a growing body of evidence that repetitive impacts can result in microhemorrhages and consequently, excessive iron deposition (Daglas and Adlard, 2018). In parallel, excessive iron deposition has been reported in several neurodegenerative diseases such as PD (Zhang et al., 2010; Barbosa

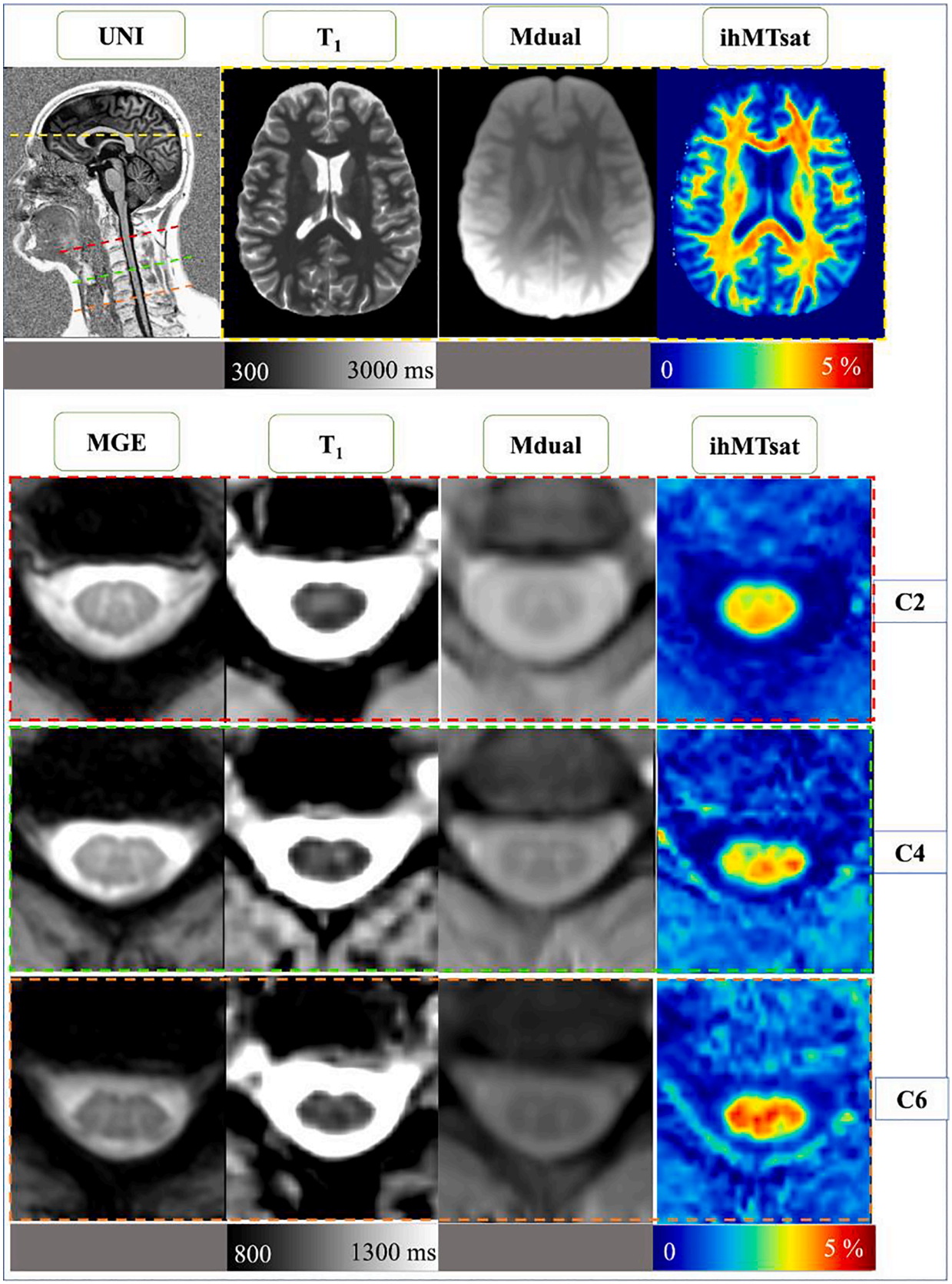

Fig. 3. Representative SC and brain images acquired on one retired rugby player (top: sagittal UNI MP2RAGE showing both brain and cervical cord; axial quantitative T_1 map, axial MT weighted image obtained with a dual-offset saturation (MT_{dual}) and corresponding ihMTsat acquired mid-brain; bottom: axial T_2*-weighted MGE, T_1 map, MT_{dual} and ihMTsat acquired at *C*2, C4 and C6 levels).

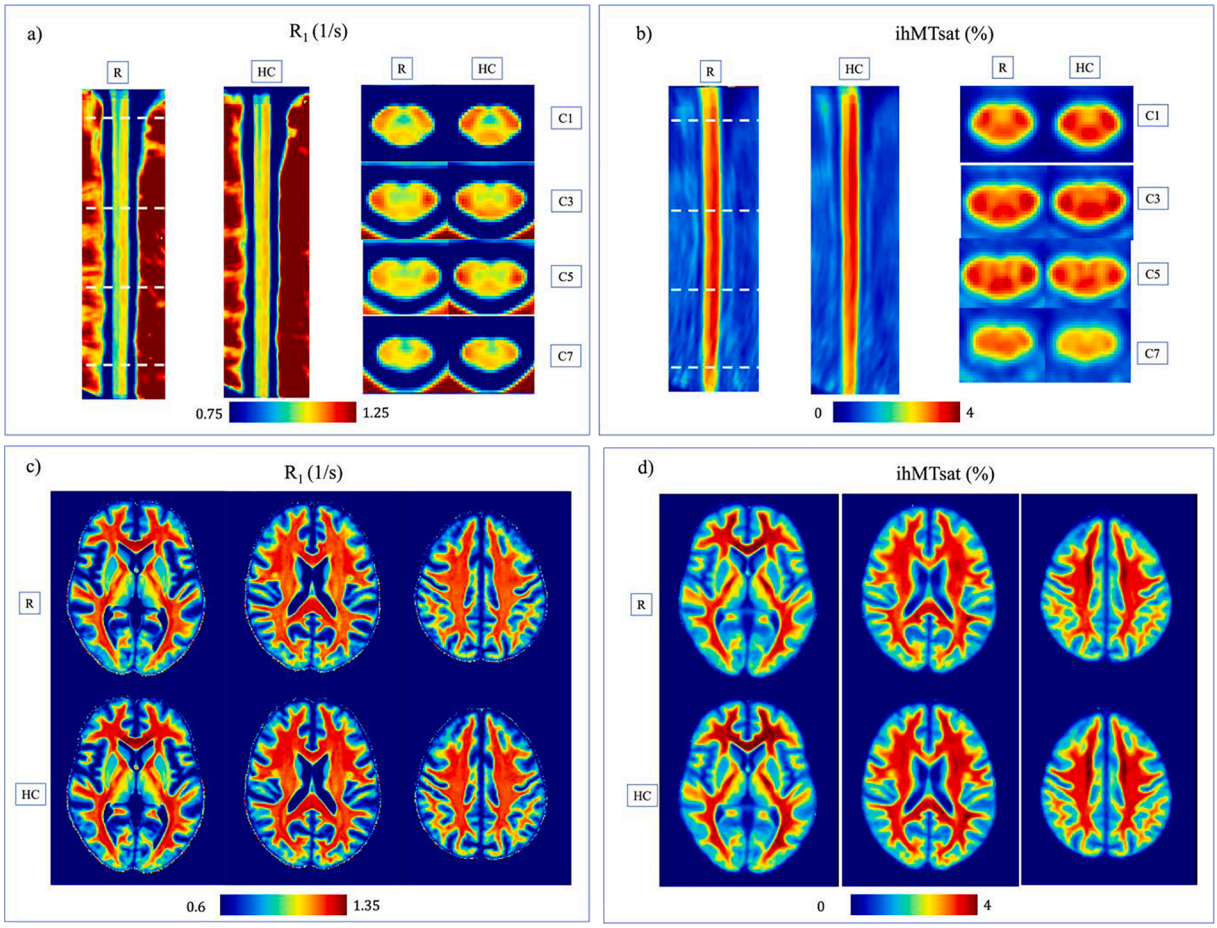

Fig. 4. (a) Mean R_1 ($1/T_1$) maps on SC, (b) mean ihMTsat maps on SC, (c) mean R_1 maps on brain, (d) mean ihMTsat maps on brain, for the 15 rugby players and 15 HC (sagittal and axial planes on SC, presented in the PAM50 space and axial planes on brain presented in MNI-152 template).

et al., 2015), MS (Bergsland et al., 2017), and Amyotrophic Lateral Sclerosis (ALS) (Oshiro et al., 2011; Kwan et al., 2012) and recent studies demonstrate that contact sports that involve repetitive head and cervical spine impacts, such as soccer and American football, could be a risk factor for ALS (Blecher et al., 2019; Chiò et al., 2009). Nonetheless, further studies using techniques sensitive to iron such as quantitative susceptibility mapping (QSM) (Mark Haacke et al., 2015) would be required to further validate this hypothesis.

Finally, when investigating the aging effect on ihMTsat values of rugby players, we observed an early decrease (in younger players as compared to HC) that could indicate demyelination and early degeneration, however, values in GM and WM then did not decrease with age as in HC, which may be linked to tissue restructuration involving microglia for instance (Loane and Byrnes, 2010). Indeed, the ihMT technique is supposedly myelin specific, however, a recent study demonstrated that ihMTsat obtained with cosine-modulated RF pulses for the dual-offset saturation (as in here) is less specific to myelination than approaches using frequency-alternated RF pulses, because non-myelin macromolecules, presumably associated with glial cells, also contribute to the ihMTsat signal (Hertanu et al., 2022). Here, microglia could thus significantly contribute to the ihMTsat value, hence counteracting the expected decrease of ihMTsat with age as a consequence of myelin loss with age. Further studies should consider this methodological aspect to possibly disentangle the different pathophysiological mechanisms.

4.3. Limitations & perspectives

This exploratory study was performed on a retired group of rugby players and the HC group was selected to match the age of players but other parameters such as profession, lifestyle, or hours of sports practice were not considered. More importantly, this investigative study was conducted on a limited number of participants and the effects should now be investigated in a larger cohort of players. Analyses based on the players experience in professional or amateur leagues could not be considered in this study due to statistical power, but similar trends were observed for both sub-populations in the cohort (data not shown). This would nonetheless require further investigations. The position of the players (forwards, especially front row, vs backs) could not be considered either due to statistical power, but such distinction would be interesting in the future. Furthermore, a longitudinal study over time and different playing seasons would allow to better delineate the short- and long-term effects of impacts. Recording impacts information such as force, moment, and linear and rotational accelerations as in (King et al., 2015; King et al., 2016; Langevin et al., 2021) would additionally enable to investigate the correlation between biomechanical forces of impacts and MRI indices of structural integrity and should be considered in the future.

Another technical limitation of this study was the spatial resolution of the ihMT technique for spinal cord imaging. The slice thickness was 10 mm to maximize SNR while keeping the acquisition time clinically acceptable (~10 min). This made the sequence prone to partial volume effect when the cord is curved (and some data had to be discarded, especially at the lower levels of the cord) and potentially less sensitive to very focal abnormalities (which were nonetheless not necessarily expected here). Note that the TR (2500 ms) could have been decreased in a normal context to accelerate the acquisition time, however, the morphology of the rugby players precludes such adjustment to stay within specific absorption rate (SAR) guidelines. This should be further

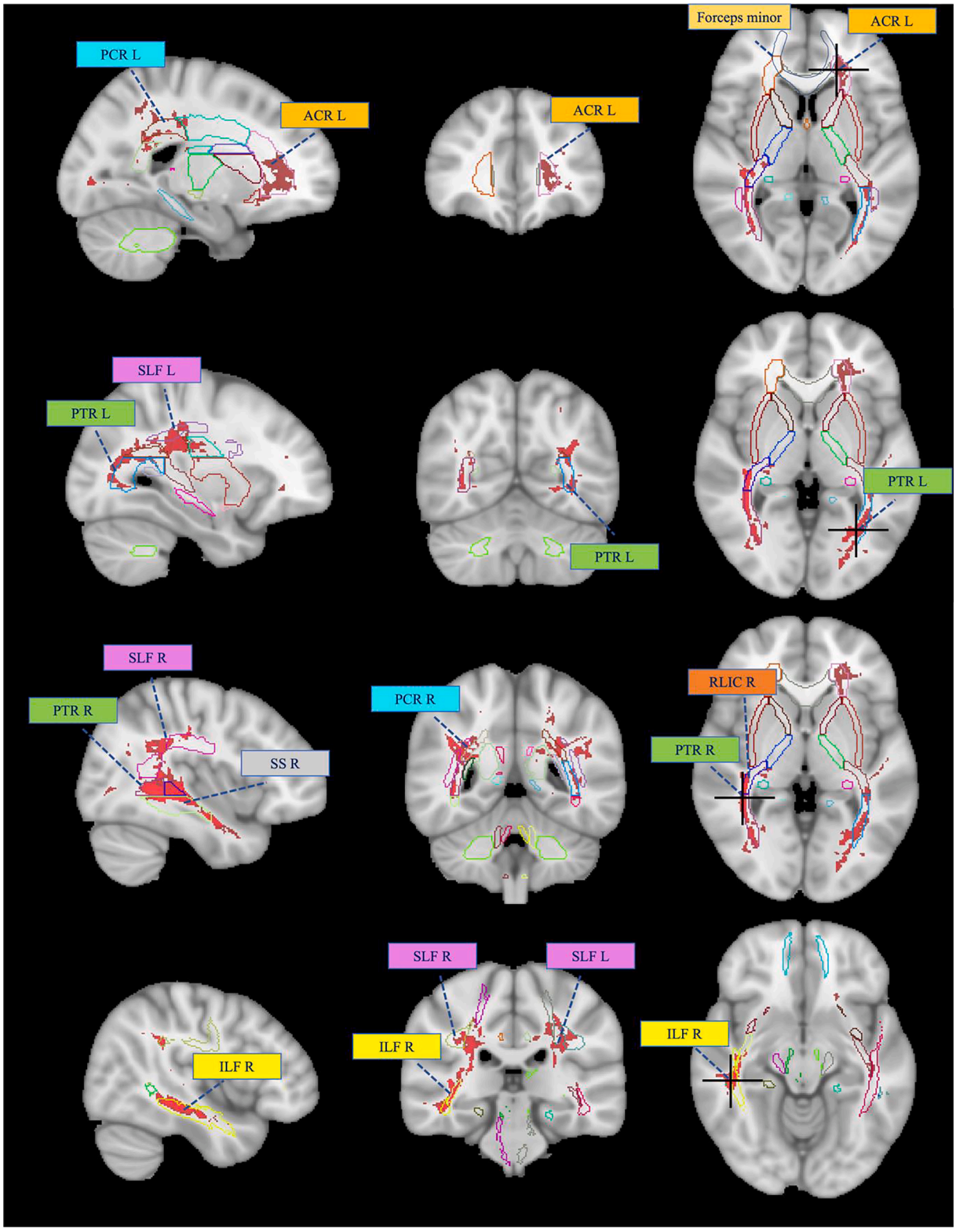

Fig. 5. Identification of the WM tracts where significant clusters from the PALM multi-variate analysis of R_1 and ihMTsat are located. The atlases used for cluster localization are JHU white-matter tractography (Wakana et al., 2007) and ICBM-DTI-81 white-matter labels atlases (Mori et al., 2008; Hua et al., 2008). The ROIs illustrated here are: ACR L: Anterior Corona Radiata L; PCR R/L: Posterior Corona Radiata Right/Left; RLIC R: Retrolenticular Limb of Internal Capsule; PTR R/L: Posterior Thalamic Radiation Right/Left; SLF R/L: Superior Longitudinal Fasciculus Right/left; SS R: Sagittal Stratum R; ILF R: Inferior Longitudinal Fasciculus Right; and Forceps minor.

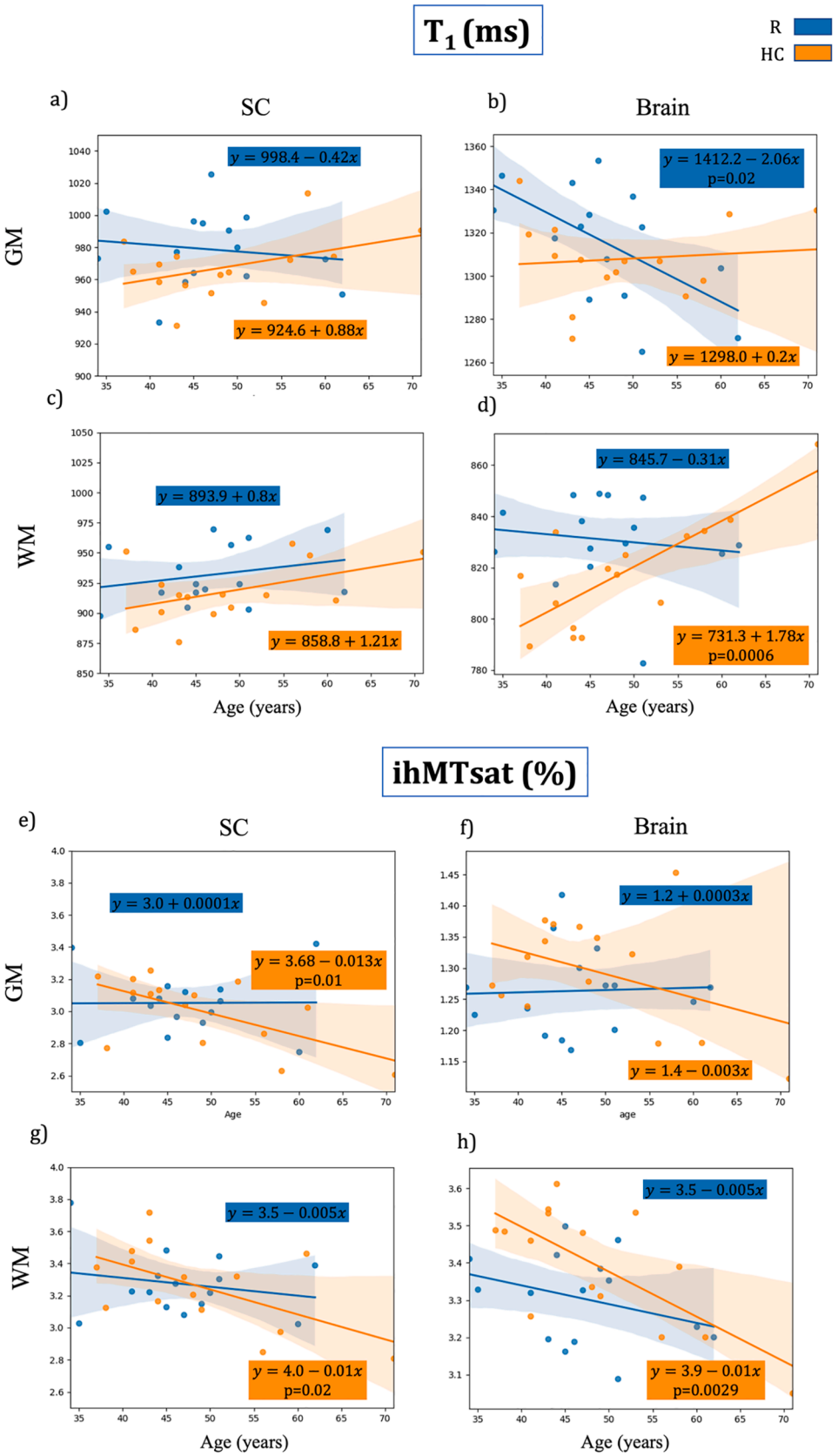

Fig. 6. Linear regression plots and equations (along with MANOVA p-value if < 0.05) for evolution of T_1 and ihMTsat with age in GM and WM of brain and SC in R (blue) and HC (orange). The T_1 in brain and SC GM decreased for rugby players with age, contrary to HC (a, b). In brain WM of rugby players, a decrease of T_1 with age together with a moderate decrease of ihMTsat as compared to HC can also be observed (d, h). Finally, values of ihMTsat in brain and SC GM remained fairly stable with age for rugby players whereas they tend to decrease for HC. GM in brain corresponds here to the whole cortical GM; WM in SC includes PST, CST, LST, and RST regions.

Table 4
Summary of all the global observations and differences between the players and HC.

Metrics	Global observations	Statistical significance	Pathophysiological hypothesis / Comments
Brain qMRI			
Multi-variate analysis using R_1 ($1/T_1$) and ihMTsat in brain WM;	Lower R_1 (higher T_1) and lower ihMTsat for players as compared to HC, in various regions such as ACR L, PCR R/L, RLIC R, PTR R/L, SLF R/L, SS R, GCC, BCC, ILF R, and Forceps minor	$p < 0.05$	Degeneration and demyelination in these specific WM tracts
T_1 in GM	Significantly decreases with age in players	$p = 0.02$	Potential iron accumulation due to micro-hemorrhages induced by repetitive impacts
T_1 in WM	Significantly increases with age in HC but not players Initial values for players above those observed in HC	$p = 0.0006$	Early aging followed by potential iron accumulation or restructuration processes
ihMTsat in WM	Significantly decreases with age in HC but not in players Initial values for players below those observed in HC	$p = 0.003$	Early aging followed by restructuration potentially involving microglia
SC qMRI			
Mean T_1 in SC GM and WM	Higher T_1 for players as compared to HC	$p < 0.05$	Diffuse degeneration in the cord, but not necessarily due to demyelination
Mean ihMTsat in SC GM and WM	Similar range in average	No	
Clinical/Morphological assessment of Spine			
Cord-to-canal ratio (CCR)	Higher trend for players on all levels (0.62 on average)	No	Slight degenerative cervical spine (without specific cord atrophy) in the range of higher risk of trauma or chronic degenerative abnormalities (Berge et al., 1999);(Castinel et al., 2010)
NDI	Higher in players than HC, but ranging from normal to mild disability	$p = 0.005$	Higher CCR but normal/mild disability in favor of efficient muscle strengthening programs and higher pain threshold in players (Brauge et al., 2015)

improved in future developments.

One should also keep in mind that the MP2RAGE technique estimates the T_1 of the tissue based on the UNI image obtained from the two RAGE volumes acquired with 2 different TIs. Although T_1 values obtained from MP2RAGE techniques have been previously validated in phantom against IR-SE (Rasoanandrianina et al., 2019), and against values reported in literature for different brain and SC regions (Forodighasemabadi et al., 2021), it is not a pure measurement of the T_1.

As mentioned in the above section, it would also be interesting to work with a frequency-alternated RF pulses ihMT sequence and combine this technique with a QSM approach in order to disentangle the different possible pathophysiological hypotheses that have been raised in this study.

Despite some limitations, and to the best of our knowledge, this study is the first to characterize cord tissue alterations in players of contact sports using quantitative MR techniques. This study is also the first investigating both brain and cSC microstructural alterations at the same time with T_1 MP2RAGE and ihMTRAGE techniques.

The techniques and post-processing tools developed in this study can now be further used to investigate microstructural alterations in other contact sports, different CNS pathologies or aging in general.

5. Conclusion

In this work, retired professional and amateur rugby players and age-matched healthy controls were recruited and studied for potential microstructural alterations of both brain and cSC using medical questionnaires and qualitative and quantitative MR techniques including T_1 relaxometry and ihMT sequences.

Higher NDI scores, higher cord-to-canal ratio, higher T_1 values suggestive of structural degeneration of cSC, together with increased T_1 and decreased ihMTsat suggestive of brain demyelination have been observed in retired rugby players as compared to age-matched controls, potentially due to cumulative effect of long-term impacts. Measurements also suggest early aging and different aging processes on brain in the players. These preliminary observations provide new insights, which should now be further investigated on larger cohorts and multicentric longitudinal studies and further correlated to the likelihood of neurodegenerative diseases (Daglas and Adlard, 2018; Zhang et al., 2010; Barbosa et al., 2015; Bergsland et al., 2017; Oshiro et al., 2011; Kwan et al., 2012) and risk factors.

CRediT authorship contribution statement

Arash Forodighasemabadi: Conceptualization, Data curation, Formal analysis, Investigation, Methodology, Software, Validation, Visualization, Writing – original draft, Writing – review & editing. **Guillaume Baucher:** Formal analysis, Investigation, Methodology, Visualization, Writing – review & editing. **Lucas Soustelle:** Formal analysis, Methodology, Software, Writing – review & editing. **Thomas Troalen:** Methodology, Writing – review & editing. **Olivier M. Girard:** Conceptualization, Formal analysis, Methodology, Validation, Writing – review & editing. **Maxime Guye:** Project administration, Resources. **Jean-Baptiste Grisoli:** Conceptualization, Data curation, Resources. **Jean-Philippe Ranjeva:** Conceptualization, Formal analysis, Validation, Writing – review & editing. **Guillaume Duhamel:** Conceptualization, Formal analysis, Methodology, Validation, Writing – review & editing. **Virginie Callot:** Conceptualization, Data curation, Formal analysis, Funding acquisition, Investigation, Methodology, Project administration, Resources, Supervision, Validation, Visualization, Writing – review & editing.

Declaration of Competing Interest

The authors declare that they have no known competing financial interests or personal relationships that could have appeared to influence the work reported in this paper.

Data availability

Data will be made available on request.

Acknowledgements

This work was performed within a laboratory member of France Life Imaging network (grant ANR-11-INBS-0006) and was supported by the Institut Carnot Star, the ARSEP Foundation (Fondation pour l'Aide à la Recherche sur la Sclérose en Plaques) and the CNRS (Centre National de

la Recherche Scientifique). The project also received funding from the European Union's Horizon 2020 research and innovation program under the Marie Skłodowska-Curie grant agreement No713750, with the financial support of the Regional Council of Provence-Alpes-Côte d'Azur and A*MIDEX (n° ANR-11-IDEX-0001-02), funded by the Investisse-ments d'Avenir project funded by the French Government, managed by the French National Research Agency (ANR).

The authors would like to thank T. Kober from Siemens Healthcare for MP2RAGE sequence support, A. Massire for T_1 post-processing code support, as well as V. Gimenez, C. Costes, P Viout, L. Pini and MP. Ranjeva for study logistics.

Appendix A. Supplementary data

Supplementary data to this article can be found online at https://doi.org/10.1016/j.nicl.2022.103124.

References

Abbas, K., Shenk, T.E., Poole, V.N., et al., 2015. Alteration of default mode network in high school football athletes due to repetitive subconcussive mild traumatic brain injury: A resting-state functional magnetic resonance imaging study. Brain Connect. 5 (2), 91–101. https://doi.org/10.1089/brain.2014.0279.

Alexander, D.G., Shuttleworth-Edwards, A.B., Kidd, M., Malcolm, C.M., 2015. Mild traumatic brain injuries in early adolescent rugby players: Long-term neurocognitive and academic outcomes. Brain Inj. 29 (9), 1113–1125. https://doi.org/10.3109/02699052.2015.1031699.

Ashburner, J., Friston, K.J., 2005. Unified segmentation. Neuroimage. 26 (3), 839–851. https://doi.org/10.1016/j.neuroimage.2005.02.018.

Association, J.O., 1996. Japanese Orthopaedic Association assessment criteria guidelines manual. Tokyo Japanese Orthop Assoc. 46–49.

Barbosa, J.H.O., Santos, A.C., Tumas, V., et al., 2015. Quantifying brain iron deposition in patients with Parkinson's disease using quantitative susceptibility mapping, R2 and R2*. Magn Reson Imaging. 33 (5), 559–565. https://doi.org/10.1016/j.mri.2015.02.021.

Bathgate, A., Best, J.P., Craig, G., Jamieson, M., 2002. A prospective study of injuries to elite Australian rugby union players. Br J Sports Med. 36 (4), 265–269. https://doi.org/10.1136/bjsm.36.4.265.

Baucher, G., Rasoanandrianina, H., Levy, S., et al., 2021. T1 mapping for microstructural assessment of the cervical spinal cord in the evaluation of patients with degenerative cervical myelopathy. Am J Neuroradiol. 42 (7), 1348–1357. https://doi.org/10.3174/ajnr.A7157.

Berge, J., Marque, B., Vital, J.M., Sénégas, J., Caillé, J.M., 1999. Age-related changes in the cervical spines of front-line rugby players. Am J Sports Med. 27 (4), 422–429. https://doi.org/10.1177/03635465990270040401.

Bergsland, N., Tavazzi, E., Laganà, M.M., et al., 2017. White Matter Tract Injury is Associated with Deep Gray Matter Iron Deposition in Multiple Sclerosis. J Neuroimaging. 27 (1), 107–113. https://doi.org/10.1111/jon.12364.

Blecher, R., Elliott, M.A., Yilmaz, E., et al., 2019. Contact Sports as a Risk Factor for Amyotrophic Lateral Sclerosis: A Systematic Review. Glob Spine J. 9 (1), 104–118. https://doi.org/10.1177/2192568218813916.

Brauge, D., Delpierre, C., Adam, P., Sol, J.C., Bernard, P., Roux, F.E., 2015. Clinical and radiological cervical spine evaluation in retired professional rugby players. J Neurosurg Spine. 23 (5), 551–557. https://doi.org/10.3171/2015.1.SPINE14594.

Castinel, B.H., Adam, P., Milburn, P.D., et al., 2010. Epidemiology of cervical spine abnormalities in asymptomatic adult professional rugby union players using static and dynamic MRI protocols: 2002 to 2006. Br J Sports Med. 44 (3), 194–199. https://doi.org/10.1136/bjsm.2007.045815.

Chiò, A., Calvo, A., Dossena, M., Ghiglione, P., Mutani, R., Mora, G., 2009. ALS in Italian professional soccer players: The risk is still present and could be soccer-specific. Amyotroph Lateral Scler. 10 (4), 205–209. https://doi.org/10.1080/17482960902721634.

Chung, S., Kim, D., Breton, E., Axel, L., 2010. Rapid B1+ mapping using a preconditioning RF pulse with turboFLASH readout. Magn Reson Med. 64 (2), 439–446. https://doi.org/10.1017/S1355771817000310.

Daglas, M., Adlard, P.A., 2018. The Involvement of Iron in Traumatic Brain Injury and Neurodegenerative Disease. Front Neurosci. 12 (December) https://doi.org/10.3389/fnins.2018.00981.

De Leener, B., Lévy, S., Dupont, S.M., et al., October 2016. SCT: Spinal Cord Toolbox, an open-source software for processing spinal cord MRI data. Neuroimage. 2017 (145), 24–43. https://doi.org/10.1016/j.neuroimage.2016.10.009.

De Leener, B., Fonov, V.S., Collins, D.L., Callot, V., Stikov, N., Cohen-Adad, J., July 2017. PAM50: Unbiased multimodal template of the brainstem and spinal cord aligned with the ICBM152 space. Neuroimage. 2018 (165), 170–179. https://doi.org/10.1016/j.neuroimage.2017.10.041.

del C. Valdés Hernández M, Ritchie S, Glatz A, et al. Brain iron deposits and lifespan cognitive ability. *Age (Omaha)*. 2015;37(5). doi:10.1007/s11357-015-9837-2.

Demortière, S., Lehmann, P., Pelletier, J., Audoin, B., Callot, V., 2020. Improved cervical cord lesion detection with 3D-MP2RAGE sequence in patients with multiple sclerosis. Am J Neuroradiol. 41 (6), 1131–1134. https://doi.org/10.3174/ajnr.A6567.

Duhamel, G., Prevost, V.H., Cayre, M., et al., 2019. Validating the sensitivity of inhomogeneous magnetization transfer (ihMT) MRI to myelin with fluorescence microscopy. Neuroimage. 199 (May), 289–303. https://doi.org/10.1016/j.neuroimage.2019.05.061.

Ercan, E., Varma, G., Mädler, B., et al., 2018. Microstructural correlates of 3D steady-state inhomogeneous magnetization transfer (ihMT) in the human brain white matter assessed by myelin water imaging and diffusion tensor imaging. Magn Reson Med. 80 (6), 2402–2414. https://doi.org/10.1002/mrm.27211.

Fonov, V., Evans, A., McKinstry, R., Almli, C., Collins, D., 2009. Unbiased nonlinear average age-appropriate brain templates from birth to adulthood. Neuroimage. 47, S102. https://doi.org/10.1016/s1053-8119(09)70884-5.

Fonov, V., Evans, A.C., Botteron, K., Almli, C.R., McKinstry, R.C., Collins, D.L., 2011. Unbiased average age-appropriate atlases for pediatric studies. Neuroimage. 54 (1), 313–327. https://doi.org/10.1016/j.neuroimage.2010.07.033.

Forodighasemabadi, A., Troalen, T., Soustelle, L., Duhamel, G., Girard, O., Callot, V., 2020:p.1175.. Towards minimal T1 and B1 contributions in cervical spinal cord inhomogeneous magnetization transfer imaging. In: *Proceedings 29th Scientific Meeting, International Society for Magnetic Resonance in Medicine*.

Forodighasemabadi, A., Rasoanandrianina, H., El Mendili, M.M., Guye, M., Callot, V., 2021. An optimized MP2RAGE sequence for studying both brain and cervical spinal cord in a single acquisition at 3T. Magn Reson Imaging. 84 (September), 18–26. https://doi.org/10.1016/j.mri.2021.08.011.

Geeraert, B.L., Lebel, R.M., Mah, A.C., et al., May 2017. A comparison of inhomogeneous magnetization transfer, myelin volume fraction, and diffusion tensor imaging measures in healthy children. Neuroimage. 2018 (182), 343–350. https://doi.org/10.1016/j.neuroimage.2017.09.019.

Girard, O.M., Prevost, V.H., Varma, G., Cozzone, P.J., Alsop, D.C., Duhamel, G., 2015. Magnetization transfer from inhomogeneously broadened lines (ihMT): Experimental optimization of saturation parameters for human brain imaging at 1.5 Tesla. Magn Reson Med. 73 (6), 2111–2121. https://doi.org/10.1002/mrm.25330.

Girard, O.M., Callot, V., Prevost, V.H., et al., 2017. Magnetization transfer from inhomogeneously broadened lines (ihMT): Improved imaging strategy for spinal cord applications. Magn Reson Med. 77 (2), 581–591. https://doi.org/10.1002/mrm.26134.

Haacke, E.M., Cheng, N.Y.C., House, M.J., et al., 2005. Imaging iron stores in the brain using magnetic resonance imaging. Magn Reson Imaging. 23 (1), 1–25. https://doi.org/10.1016/j.mri.2004.10.001.

Hagemeier, J., Geurts, J.J.G., Zivadinov, R., 2012. Brain iron accumulation in aging and neurodegenerative disorders. Expert Rev Neurother. 12 (12), 1467–1480. https://doi.org/10.1586/ern.12.128.

Harris, F.J., 1978. On the Use of Windows for Harmonic Analysis with the Discrete Fourier Transform. Proc IEEE. 66 (1), 51–83. https://doi.org/10.1109/PROC.1978.10837.

Helms, G., Dathe, H., Kallenberg, K., Dechent, P., 2008. High-resolution maps of magnetization transfer with inherent correction for RF inhomogeneity and T1 relaxation obtained from 3D FLASH MRI. Magn Reson Med. 60 (6), 1396–1407. https://doi.org/10.1002/mrm.21732.

Hertanu, A., Soustelle, L., Le Troter, A., et al., 2022. T 1D -weighted ihMT imaging – Part I. Isolation of long- and short-T 1D components by T 1D -filtering. Magn Reson Med. 87 (5), 2313–2328. https://doi.org/10.1002/mrm.29139.

Hua, K., Zhang, J., Wakana, S., et al., 2008. Tract probability maps in stereotaxic spaces: Analyses of white matter anatomy and tract-specific quantification. Neuroimage. 39 (1), 336–347. https://doi.org/10.1016/j.neuroimage.2007.07.053.

Hume, P.A., Theadom, A., Lewis, G.N., et al., 2017. A Comparison of Cognitive Function in Former Rugby Union Players Compared with Former Non-Contact-Sport Players and the Impact of Concussion History. Sport Med. 47 (6), 1209–1220. https://doi.org/10.1007/s40279-016-0608-8.

Jäncke, L., Mérillat, S., Liem, F., Hänggi, J., 2015. Brain size, sex, and the aging brain. Hum Brain Mapp. 36 (1), 150–169. https://doi.org/10.1002/hbm.22619.

King, D., Hume, P.A., Brughelli, M., Gissane, C., 2015. Instrumented mouthguard acceleration analyses for head impacts in amateur rugby union players over a season of matches. Am J Sports Med. 43 (3), 614–624. https://doi.org/10.1177/0363546514560876.

King, D.A., Hume, P.A., Gissane, C., Clark, T.N., 2016. Similar head impact acceleration measured using instrumented ear patches in a junior rugby union team during matches in comparison with other sports. J Neurosurg Pediatr. 18 (1), 65–72. https://doi.org/10.3171/2015.12.PEDS15605.

Kober, T., Granziera, C., Ribes, D., et al., 2012. MP2RAGE multiple sclerosis magnetic resonance imaging at 3 T. Invest Radiol. 47 (6), 346–352. https://doi.org/10.1097/RLI.0b013e31824600e9.

Koerte, I.K., Kaufmann, D., Hartl, E., et al., 2012. A prospective study of physician-observed concussion during a varsity university hockey season: white matter integrity in ice hockey players. Part 3 of 4. Neurosurg Focus. 33 (6), 1–7.

Kwan, J.Y., Jeong, S.Y., van Gelderen, P., et al., 2012. Iron accumulation in deep cortical layers accounts for MRI signal abnormalities in ALS: Correlating 7 tesla MRI and pathology. PLoS One. 7 (4) https://doi.org/10.1371/journal.pone.0035241.

Langevin, T.L., Antonoff, D., Renodin, C., et al., 2021. Head impact exposures in women's collegiate rugby. Phys Sportsmed. 49 (1), 68–73. https://doi.org/10.1080/00913847.2020.1770568.

Loane, D.J., Byrnes, K.R., 2010. Role of Microglia in Neurotrauma. Neurotherapeutics. 7 (4), 366–377. https://doi.org/10.1016/j.nurt.2010.07.002.

Manning KY, Brooks JS, Dickey JP, et al. Longitudinal changes of brain microstructure and function in nonconcussed female rugby players. *Neurology*. 2020;95(4):E402-E412. doi:10.1212/WNL.0000000000009821.

Mark Haacke, E., Reichenbach, J.R., Wang, Y., 2015. Susceptibility-Weighted Imaging and Quantitative Susceptibility Mapping. Brain Mapp An Encycl Ref. 1 (1), 161–172. https://doi.org/10.1016/B978-0-12-397025-1.00019-1.

Marques, J.P., Gruetter, R., 2013. New Developments and Applications of the MP2RAGE Sequence - Focusing the Contrast and High Spatial Resolution R1 Mapping. PLoS One. 8 (7), e69294.

Marques, J.P., Kober, T., Krueger, G., van der Zwaag, W., Van de Moortele, P.F., Gruetter, R., 2010. MP2RAGE, a self bias-field corrected sequence for improved segmentation and T1-mapping at high field. Neuroimage. 49 (2), 1271–1281. https://doi.org/10.1016/j.neuroimage.2009.10.002.

Massire, A., Taso, M., Besson, P., Guye, M., Ranjeva, J.P., Callot, V., 2016. High-resolution multi-parametric quantitative magnetic resonance imaging of the human cervical spinal cord at 7T. Neuroimage. 143, 58–69. https://doi.org/10.1016/j.neuroimage.2016.08.055.

Mchinda, S., Varma, G., Prevost, V.H., et al., 2018. Whole brain inhomogeneous magnetization transfer (ihMT) imaging: Sensitivity enhancement within a steady-state gradient echo sequence. Magn Reson Med. 79 (5), 2607–2619. https://doi.org/10.1002/mrm.26907.

Mori, S., Oishi, K., Jiang, H., et al., 2008. Stereotaxic white matter atlas based on diffusion tensor imaging in an ICBM template. Neuroimage. 40 (2), 570–582. https://doi.org/10.1016/j.neuroimage.2007.12.035.

Munsch, F., Varma, G., Taso, M., et al., October 2020. Characterization of the cortical myeloarchitecture with inhomogeneous Magnetization Transfer imaging (ihMT). Neuroimage. 2020 (225), 117442 https://doi.org/10.1016/j.neuroimage.2020.117442.

Núñez, M.T., Urrutia, P., Mena, N., Aguirre, P., Tapia, V., Salazar, J., 2012. Iron toxicity in neurodegeneration. BioMetals. 25 (4), 761–776. https://doi.org/10.1007/s10534-012-9523-0.

Okubo, G., Okada, T., Yamamoto, A., et al., 2016. MP2RAGE for deep gray matter measurement of the brain: A comparative study with MPRAGE. J Magn Reson Imaging. 43 (1), 55–62. https://doi.org/10.1002/jmri.24960.

Oshiro, S., Morioka, M.S., Kikuchi, M., 2011. Dysregulation of iron metabolism in Alzheimer's disease, Parkinson's disease, and amyotrophic lateral sclerosis. Adv Pharmacol Sci. 2011 https://doi.org/10.1155/2011/378278.

Patenaude, B., Smith, S.M., Kennedy, D.N., Jenkinson, M., 2011. A Bayesian model of shape and appearance for subcortical brain segmentation. Neuroimage. 56 (3), 907–922. https://doi.org/10.1016/j.neuroimage.2011.02.046.

Paul, F., 2016. Pathology and MRI: exploring cognitive impairment in MS. Acta Neurol Scand. 134 (July), 24–33. https://doi.org/10.1111/ane.12649.

Prevost, V.H., Girard, O.M., Varma, G., Alsop, D.C., Duhamel, G., 2016. Minimizing the effects of magnetization transfer asymmetry on inhomogeneous magnetization transfer (ihMT) at ultra-high magnetic field (11.75 T). Magn Reson Mater Physics, Biol Med. 29 (4), 699–709. https://doi.org/10.1007/s10334-015-0523-2.

Prevost, V.H., Girard, O.M., Mchinda, S., Varma, G., Alsop, D.C., Duhamel, G., 2017. Optimization of inhomogeneous magnetization transfer (ihMT) MRI contrast for preclinical studies using dipolar relaxation time (T1D) filtering. NMR Biomed. 30 (6), 1–13. https://doi.org/10.1002/nbm.3706.

Rangwala, N., Varma, G., Hackney, D., Alsop, D.C., 2013:p.350.. Quantification of myelin in the cervical spinal cord using inhomogeneous magnetization transfer imaging. In: *Proceedings 21st Scientific Meeting, International Society for Magnetic Resonance in Medicine*.

Rasoanandrianina, H., 2019. Toward the characterization of macro and micro -traumatisms of the human cervical spinal cord in rugby. PhD Thesis.

Rasoanandrianina H, Duhamel G, Feiweier T, et al. Regional and structural integrity of the whole cervical spinal cord using 3D-T1 MP2RAGE and multi-slice multi angle DTI and ihMT sequences at 3T : preliminary investigations on age-related changes . In: *Proceedings 25th Scientific Meeting, International Society for Magnetic Resonance in Medicine*. ; 2017:p.0912.

Rasoanandrianina, H., Massire, A., Taso, M., et al., 2019. Regional T1 mapping of the whole cervical spinal cord using an optimized MP2RAGE sequence. NMR Biomed. 32 (11), 1–17. https://doi.org/10.1002/nbm.4142.

Rasoanandrianina, H., Demortière, S., Trabelsi, A., et al., 2020. Sensitivity of the Inhomogeneous Magnetization Transfer Imaging Technique to Spinal Cord Damage in Multiple Sclerosis. AJNR Am J Neuroradiol. 41 (5), 929–937. https://doi.org/10.3174/ajnr.A6554.

Shuttleworth-Rdwards, A.B., Radloff, S.E., 2008. Compromised visuomotor processing speed in players of Rugby Union from school through to the national adult level. Arch Clin Neuropsychol. 23 (5), 511–520. https://doi.org/10.1016/j.acn.2008.05.002.

Sian-Hülsmann, J., Mandel, S., Youdim, M.B.H., Riederer, P., 2011. The relevance of iron in the pathogenesis of Parkinson's disease. J Neurochem. 118 (6), 939–957. https://doi.org/10.1111/j.1471-4159.2010.07132.x.

Simioni, S., Amarù, F., Bonnier, G., et al., 2014. MP2RAGE provides new clinically-compatible correlates of mild cognitive deficits in relapsing-remitting multiple sclerosis. J Neurol. 261 (8), 1606–1613. https://doi.org/10.1007/s00415-014-7398-4.

Soustelle, L., Lamy, J., Le Troter, A., et al., 2020. A Motion Correction Strategy for Multi-Contrast based 3D parametric imaging : Application to Inhomogeneous Magnetization Transfer (ihMT). bioRxiv. https://doi.org/10.1101/2020.09.11.292649.

Stamm, J.M., Koerte, I.K., Muehlmann, M., et al., 2015. Age at First Exposure to Football Is Associated with Altered Corpus Callosum White Matter Microstructure in Former Professional Football Players. J Neurotrauma. 32 (22), 1768–1776. https://doi.org/10.1089/neu.2014.3822.

Stüber, C., Morawski, M., Schäfer, A., et al., 2014. Myelin and iron concentration in the human brain: A quantitative study of MRI contrast. Neuroimage. 93 (P1), 95–106. https://doi.org/10.1016/j.neuroimage.2014.02.026.

Taki, Y., Thyreau, B., Kinomura, S., et al., 2011. Correlations among brain gray matter volumes, age, gender, and hemisphere in healthy individuals. PLoS One. 6 (7), e22734.

Taso, M., Girard, O.M., Duhamel, G., et al., 2016. Tract-specific and age-related variations of the spinal cord microstructure: A multi-parametric MRI study using diffusion tensor imaging (DTI) and inhomogeneous magnetization transfer (ihMT). NMR Biomed. 29 (6), 817–832. https://doi.org/10.1002/nbm.3530.

Troalen T, Callot V, Varma G, Guye M, Alsop DC, Girard OM. Cervical Spine inhomogeneous Magnetization Transfer (ihMT) Imaging Using ECG-Triggered 3D Rapid Acquisition Gradient-Echo (ihMT-RAGE). In: *Proceedings 27th Scientific Meeting, International Society for Magnetic Resonance in Medicine*. ; 2018:p.300.

Van Obberghen, E., Mchinda, S., Le Troter, A., et al., 2018. Evaluation of the sensitivity of inhomogeneous magnetization transfer (ihMT) MRI for multiple sclerosis. Am J Neuroradiol. 39 (4), 634–641. https://doi.org/10.3174/ajnr.A5563.

Varma G, Munsch F, Burns B, et al. Three-dimensional inhomogeneous magnetization transfer with rapid gradient-echo (3D ihMTRAGE) imaging. *Magn Reson Med*. 2020;(April):mrm.28324. doi:10.1002/mrm.28324.

Varma, G., Girard, O.M., Prevost, V.H., Grant, A.K., Duhamel, G., Alsop, D.C., 2015. Interpretation of magnetization transfer from inhomogeneously broadened lines (ihMT) in tissues as a dipolar order effect within motion restricted molecules. J Magn Reson. 260, 67–76. https://doi.org/10.1016/j.jmr.2015.08.024.

Varma, G., Duhamel, G., De Bazelaire, C., Alsop, D.C., 2015. Magnetization transfer from inhomogeneously broadened lines: A potential marker for myelin. Magn Reson Med. 73 (2), 614–622. https://doi.org/10.1002/mrm.25174.

Varma, G., Girard, O.M., Mchinda, S., et al., 2018. Low duty-cycle pulsed irradiation reduces magnetization transfer and increases the inhomogeneous magnetization transfer effect. J Magn Reson. 296, 60–71. https://doi.org/10.1016/j.jmr.2018.08.004.

Varma G, Munsch F, Girard OM, Duhamel G, Alsop DC. An inhomogeneous magnetization transfer (ihMT) quantification method robust to B1 and T1 variations in magnetization prepared acquisitions. In: *Proceedings 27th Scientific Meeting, International Society for Magnetic Resonance in Medicine*. ; 2019:p.4911.

Vernon, H., Mior, S., 1991. The neck disability index: A study of reliability and validity. J Manipulative Physiol Ther. 14 (7), 409–415.

Wakana, S., Caprihan, A., Panzenboeck, M.M., et al., 2007. Reproducibility of quantitative tractography methods applied to cerebral white matter. Neuroimage. 36 (3), 630–644. https://doi.org/10.1016/j.neuroimage.2007.02.049.

Winkler, A.M., Ridgway, G.R., Webster, M.A., Smith, S.M., Nichols, T.E., 2014. Permutation inference for the general linear model. Neuroimage. 92, 381–397. https://doi.org/10.1016/j.neuroimage.2014.01.060.

Winkler, A.M., Webster, M.A., Brooks, J.C., Tracey, I., Smith, S.M., Nichols, T.E., 2016. Non-parametric combination and related permutation tests for neuroimaging. Hum Brain Mapp. 37 (4), 1486–1511. https://doi.org/10.1002/hbm.23115.

Zhang, J., Zhang, Y., Wang, J., et al., 2010. Characterizing iron deposition in Parkinson's disease using susceptibility-weighted imaging: An in vivo MR study. Brain Res. 1330, 124–130. https://doi.org/10.1016/j.brainres.2010.03.036.